

Received April 10, 2017, accepted April 27, 2017, date of publication May 2, 2017, date of current version June 28, 2017.

Digital Object Identifier 10.1109/ACCESS.2017.2699970

Analytical Model of Spread of Epidemics in Open Finite Regions

DAXIN TIAN¹, (Senior Member, IEEE), CHAO LIU¹, ZHENGGUO SHENG²,
MIN CHEN³, (Senior Member, IEEE), AND YUNPENG WANG¹

¹Beijing Key Laboratory for Cooperative Vehicle Infrastructure Systems and Safety Control, School of Transportation Science and Engineering, Beihang University, Beijing 100191, China

²Department of Engineering and Design, University of Sussex, Richmond 3A09, U.K.

³School of Computer Science and Technology, Huazhong University of Science and Technology, Wuhan 430074, China

Corresponding author: Min Chen (minchen2012@hust.edu.cn)

This work was supported in part by the National Natural Science Foundation of China under Grant 61672082 and Grant U1564212, in part by The Engineering and Physical Sciences Research Council under Grant EP/P025862/1, in part by the Royal Society-Newton Mobility Grant under Grant IE160920, and in part by the Asa Briggs Visiting Fellowship from the University of Sussex.

ABSTRACT Epidemic dynamics, a kind of biological mechanisms describing microorganism propagation within populations, can inspire a wide range of novel designs of engineering technologies, such as advanced wireless communication and networking, global immunization on complex systems, and so on. There have been many studies on epidemic spread, but most of them focus on closed regions where the population size is fixed. In this paper, we proposed a susceptible–exposed–infected–recovered model with a variable contact rate to depict the dynamic spread processes of epidemics among heterogeneous individuals in open finite regions. We took the varied number of individuals and the dynamic migration rate into account in the model. We validated the effectiveness of our proposed model by simulating epidemics spread in different scenarios. We found that the average infected possibility of individuals, the population size of infectious individuals in the regions, and the infection ability of epidemics have great impact on the outbreak sizes of epidemics. The results demonstrate that the proposed model can well describe epidemics spread in open finite regions.

INDEX TERMS Epidemic dynamics, spreading behavior, system model.

I. INTRODUCTION

Recently, epidemic spreading mechanism has inspired effective and robust solutions for a variety of engineering issues, ranging from wireless communication and networking, social health management [1], network virus prevention, etc. For example, epidemic dynamics has motivated Tian et al. to develop an energy-efficient vehicular beaconing control strategy [2] as well as a highly efficient and reliable vehicular routing protocol [3]. References [4] and [5] have applied a basic epidemic model to investigate information propagation over computer networks and other general distributed systems. Many other studies on global immunization strategies over complex systems and on distributed information controls in cyber spaces are also based on well-formulated epidemic spreading models [6], [7]. Epidemic-inspired designs are appealing and believed to go far beyond many conventional engineering approaches, so it is of great significance to give a deep insight into the biological mechanism through proper mathematical models as well as computer simulations. With respect to epidemic spread, there exist a great quantity

of researches, and the susceptible–infectious–susceptible (SIS) and susceptible–infectious–recovered (SIR) models are the most extensively studied [8].

Existing research on the spread of epidemics can be classified into two types, namely individual and population levels. As research on epidemic spread becomes more in depth, an increasing number of factors are taken into account. As is well known, vaccination can mitigate epidemic spread and is one of the most effective tools for reducing morbidity and mortality [9]. Researchers have also found that age, sex, and temperature influence epidemic outbreak and spread [10]–[12]. In addition, the diversity of human mobility patterns and individual behaviours has a significant influence on the spreading processes of infectious diseases [13], [14], for example, the use of a mask can reduce the probability of an individual being infected. Furthermore, many approaches have been used to investigate the spread of epidemics. Agent-based models [15] can be used to study the spreading processes of epidemics in local areas, and metapopulation models can be used to investigate the

global spread of epidemics [16]–[18]. In particular, complex networks can express the heterogeneity of interactions characteristic of many human activities [19], [20] and have become a very important approach for describing the spread of epidemics [21]. It is worth noting that 1) a metapopulation model is a type of network and 2) complex networks can be used to investigate the spread of epidemics both locally and globally. Single-layer networks are powerful tools for studying the spread of individual epidemics, and multilayer networks can be used to investigate more complex scenarios [22]; for example, infectious diseases spread along with information broadcasting [23], and even different kinds of pathogens spread spatially in competition [24]. In addition, many researchers have made use of data from mobile phones, airline networks, and commuting networks to study the relationship between travel networks and epidemic spread [22], [25]–[30]. Investigators have also found that the reproduction number and epidemic threshold play very important roles in the spreading processes of infectious diseases and might provide a basis for containing epidemics [31], [32].

At present, the rapid development of modern means of transportation enables people to travel globally and more frequently than previously, and it is more likely that an epidemic outbreak in a local region might spread around the world and threaten international public health [33]; for example, severe acute respiratory syndrome (SARS), which broke out in China in 2003, spread across much of the globe and caused thousands of deaths. Many researchers have used metapopulation models to analyze epidemic spread on a global scale. On the other hand, it is easier for a large number of people to assemble in open finite regions, such as transport hubs and mass gathering venues. Nevertheless, there are few studies focusing on epidemic spread in these regions. Generally, the spread of epidemics in open finite regions may be faster than that in other places because of the high density and high mobility of people in these regions. So it is necessary to study how the epidemics spread in these regions. A number of studies reveal that human mobility in finite regions is dynamic, self-adaptive, and self-organizing [34]. Investigating the spreading processes of epidemics in an open finite region can be more complex, because the number and density of people in the region may vary as people enter and leave. In addition, the heterogeneous lengths of time that individuals remain in such a region also impact the possibility of being infected [35]. Conventional SIS or SIR models assume that 1) the population size is constant. This means those models do not consider the mobility of people, so they cannot be used to study the epidemic spread in the open regions. 2) The individuals are homogeneous, which means such an approach neglects the heterogeneous social interaction and mobility patterns of people. 3) The individuals in the population are well mixed. To the best of our knowledge, the existing literature on epidemic spread does not take varying numbers and densities of people into account simultaneously. Hence, the existing approaches are difficult to use to describe the spread

processes of epidemics in the open finite regions where the number and density of people might change over time.

In this paper, we presented an analytical model to analyze the spread processes of epidemics in open finite regions. Since the mobility of people, the number and the density of people change, which has been shown to have significant influence on the epidemics spread [14]. So in our model, we took the varied number and density of individuals into account simultaneously, and we also considered the dynamic migration process of individuals. We validated the validity of the analytical model through simulating epidemics spread in different scenarios. We found that the outbreak size of an epidemic in open finite regions is mainly determined by 1) the average infected possibility of individuals, 2) the infection ability of the epidemic, and 3) the number of the infectious individuals who are in the region. Moreover, not all of the susceptible individuals in the open regions are infected due to the mobility of individuals. Most importantly, the results show that the proposed model can well describe epidemics spread in open finite regions. The analytical model may provide a way to predict the outbreak size of epidemics in open regions.

II. TIME-CONTINUOUS SEIR MODEL WITH MOBILITY

Though complex networks with heterogeneous connectivity are powerful tools for describing the spread of epidemics, it cannot be used to study the dynamic spread processes of epidemics in the open finite regions, such as emporiums, schools and transport hubs, because it is difficult to obtain the degree distribution in such highly dynamic environment. In this paper, we presented an analytical model to describe the spread processes of epidemics in such regions. We considered epidemic spread in a region (the acreage of the region is A), in which the number of individuals at time t is $N(t)$. Each individual is in one of four states: 1) susceptible, S ; 2) exposed, E ; 3) infectious, I ; or 4) recovered, R . Among the individuals, the proportions of susceptible, exposed, and infectious individuals are $s(t)$, $e(t)$, and $i(t)$, respectively. A susceptible individual can enter the exposed state when infected by infectious individuals. Individuals in the exposed state cannot infect the susceptible individuals, but they will enter the infectious state after a latent period. After a period of time, the infectious individuals will recover due to the body immunity, i.e., change from I to R . The individuals in recovered state are not infected any more. In reality, some people may take preventive measures (such as using masks) to reducing the possibility that they are infected by the epidemics. As people are heterogeneous, the sensitivities of them to the epidemics are different. So the individuals have different possibilities to be infected by epidemics. We used a parameter p ($0 < p \leq 1$) to denote the average probability that the individuals are infected by the epidemics. We assumed the possibility that an exposed individual enters the infectious state is γ , and the possibility that an infectious individual enters the recovered state is μ . Since individuals can enter and leave the region, we defined that the arrival and departure

rates of individuals at time t are $\alpha(t)$ and $\beta(t)$, respectively. Among the arrival individuals, the proportions of susceptible, exposed, and infectious individuals are $s'(t)$, $e'(t)$, and $i'(t)$, respectively. According to the assumptions above, we thus obtained the time-continuous SEIR model described by the following differential equations:

$$\frac{ds(t)}{dt} = -p\lambda i(t)s(t) + \frac{\alpha(t)}{N(t)}[s'(t) - s(t)] \quad (1)$$

$$\frac{de(t)}{dt} = p\lambda i(t)s(t) + \frac{\alpha(t)}{N(t)}[e'(t) - e(t)] - \gamma e(t) \quad (2)$$

$$\frac{di(t)}{dt} = \gamma e(t) + \frac{\alpha(t)}{N(t)}[i'(t) - i(t)] - \mu i(t) \quad (3)$$

In the above equations, λ is the contact rate [36]. Our model inherits the assumption that the individuals in the region are well mixed from the conventional SIR models. Since this assumption was made, the differential equations do not include the departure rate $\beta(t)$, which demonstrates that the departure rate does not influence the epidemic spreading under this assumption. It is worth noting that the time people remain in some places, such as airports and railway stations, is relatively limited (much shorter than the latent period of epidemic), and the exposed individuals cannot enter the infectious state in such limited time. In this case, we can just consider the process that susceptible individuals enter the exposed state when they are infected by infectious individuals. And then the SEIR model can be simplified to the SEI model by setting γ and μ to zero.

A. CONTACT RATE

In epidemic spread models, the contact rate is a very important parameter, which can reflect the infection intensity of an epidemic. In most of the existing literature, the number of individuals was assumed to be constant and thus the contact rate was also regarded as constant. However, in reality the contact rate can vary as people move. Studies show that the moving of people in a finite region is complex and self-adaptive [35]. Reference [37] studied the contact rate by obtaining the distribution of the local population density. Unfortunately, the real-time density distribution is difficult to obtain in open regions due to the mobility of people. In fact, the contact rate is influenced not only by the density of the individuals, but also by the infectious radius of the epidemics; for example, sneezing can impact individuals within a range of six meters, whereas coughing can only impact individuals within a range of two meters [37]. Hu and Nigmatulina [36] found that the contact rate in reality monotonically increases with density, but saturates as density is too high because of the low moving speeds of individuals; besides, an epidemic can infect more individuals per unit time if it has a larger infection radius. They proposed a spatial contact model to describe the relationship between contact rate and the density and infection radius, and they considered the contact rate decays with distance increasing. In this paper,

we adopted the following spatial contact rate model shown in [36]:

$$\lambda(\rho) = k\pi\rho_0(1 - e^{-r^2\frac{\rho}{\rho_0}}) \quad (4)$$

In which $k(0 < k < 1)$ is a constant fraction of contacts among the individuals; $\rho = \frac{N(t)}{A}$ is the average density of the individuals in the finite region; r is the maximum infection radius of the epidemic; ρ_0 is the maximum density of individuals in the most crowded situation (where individuals could hardly move), which may be drawn from the range of $[6, 10] / \text{m}^2$ [36], [37].

B. MIGRATION RATE

In the open finite regions, the density of individuals can be changed due to the mobility of people, thereby causing the contact rate change. The change of density is determined not only by the arrival rate, but also by the departure rate. We called the arrival and departure rates as migration rate, which has substantial influence on a metapopulation model. Since people's arrival or departure is random, the real-time migration rate is also difficult to obtain. Thus, in almost all of the existing metapopulation models, the migration rate is regarded as constant to reflect the average number of individuals who enter or leave a region per unit time. In some places, it is easy to know the number of people who have gotten there in a certain period of time. For instance, scenic spots can obtain this information by counting the tickets sold in the corresponding period. In airports and railway stations, there are accurate records for the people who have reached or left there. A large number of smart card data have revealed that the number of people who reached subway stations periodically changes by the cycle of one day [38]–[40]. In this paper, we studied the spread processes of epidemics with the migration rate varying. Assume we can obtain the historical data about people mobility in a place, and we can calculate the average migration rate by the hour. According to the existing researches [38]–[40], we can further assume that the average arrival rate of each hour periodically changes by the cycle of one day, and the arrival rate (in second) of the j^{th} ($j = 0, 1, 2, \dots, 23$) hour of a day obeys the normal distribution $N(m_j, \sigma_j^2)$, herein, m_j and σ_j are the mean and standard deviation of the arrival rate of the j^{th} hour calculated by the historical data, respectively. We aggregated the hourly number of people who reached and left the Beijing Capital International Airport from January 15 to 21, 2016. The average arrival and departure rates of each hour are shown in Fig. 1. Fig. 1 shows that the arrival (departure) rate is not a constant, but periodically changes and drastically fluctuates around the average value, and the average values are much different in the different periods of time. It indicates that our assumptions are reasonable. In the simulation section, for simplicity, the arrival rate $\alpha(t)$ was drawn from the interval $[m_j - \sigma_j, m_j + \sigma_j]$ uniformly to depict the dynamic arrival process of individuals. It is worth noting that the components of the arrival individuals also influence the spreading processes

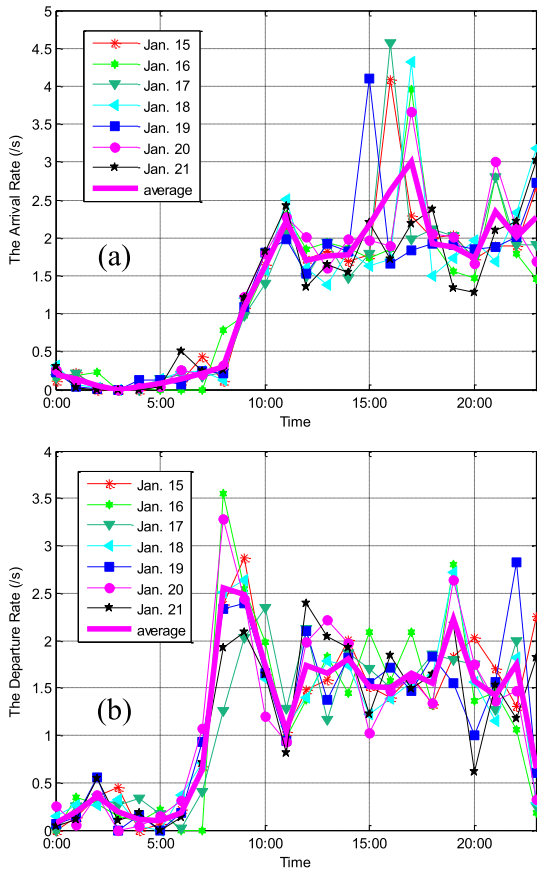


FIGURE 1. The curves were plotted in accordance with the migration rate of the Beijing Capital International Airport from January 15 to 21, 2016. The migration rate periodically changes by the cycle of one day. (a) Arrival rate. (b) Departure rate.

of epidemics; intuitively, a large $i(t)$ can accelerate epidemic spread.

III. EXPERIMENTS AND SIMULATION RESULTS

In order to validate the proposed model, we developed a simulator in MATLAB to simulate a hypothetical epidemic spreading in an open finite region as shown in Fig. 2. In our simulations, we run an agent-based model in an open finite region. The acreage of the region was 500 m² (the size was much larger than the infection range of epidemic), and it can hold x ($x = 300, 500, 800$ and 1500 , respectively) individuals at most. At the initial time t_0 , $N(t_0)$ individuals were uniformly distributed in the region. In each simulation step, $\alpha(t)$ individuals entered the region, but individuals might be forbidden from entering when the number of individuals approaches to the capacity of region. In reality, people in open finite regions, airports for example, can be simply classified into two types: some stay in the waiting room to wait for their airplanes and the others walk from the entrance to the exit directly to get on the airplanes. So in our simulation, we also divided the individuals into two groups: some moved in the region randomly based on the random direction model (RDM) [41] and the others moved from the entrance

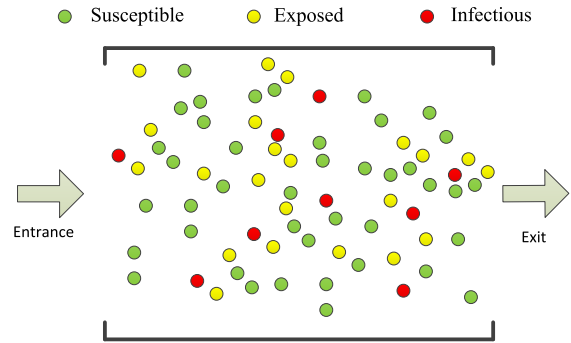


FIGURE 2. Schematic illustration of epidemic spread among individuals in open finite region. It is an agent-based model (ABM). The susceptible individuals enter exposed state when they are infected by the infectious ones.

to the exit directly. The individuals who were near the exit can leave the region, but we set the maximum departure rate to be 5/s. We preset a possibility p at the beginning of the simulation. The moving speeds of individuals were set randomly to be within the interval $[0.05, 1.34]$ m/s [31], [35]. As the individuals move, when a susceptible individual enters the infectious range of an infection individual (i.e. the distance between them is shorter than r), it generates a pseudorandom value ξ drawn from the standard uniform distribution on the open interval $(0,1)$. If $\xi \leq p$, the susceptible individual was infected and entered the exposed state; it remained its state, otherwise. The simulation time step was set to be one second, and all of the simulations last 1800 seconds. Generally, 1800s is much shorter than the latency of an epidemic, so the SEIR model can be simplified to SEI model. We modeled the epidemic spreading in different scenarios by changing the simulation settings and the simulation was repeated 100 times in each setting. And we verified the efficiency of the proposed model by comparing the analytical and simulation results. Since the differential Equations (1)-(3) have no analytic solutions, we obtained the numerical solutions by the Eulerian Method. By the way, we compared the results under different scenarios to find the main factors that impact epidemics spread. The parameters of k and ρ_0 in the contact rate were set to be $k = 0.15$ and $\rho_0 = 7$ to fit the simulation data. Detailed results are shown as follows.

Many investigations have found that preventive behaviours of people can reduce the possibility that they are infected by the epidemics. In our simulation, we set the average infected possibility of individuals to be 0.3 and 0.8 to simulate the epidemic spreading on different prevention levels, respectively. We also set the average infected possibility to be 1 to observe the extreme infection under the worst case, in which a susceptible individual is infected immediately when it encounters an infectious one. Fig. 3 shows the simulation and analytical results obtained under the three infected possibilities. In Fig. 3(a), (b), (c) and (d), we modeled the epidemic spreading among the individuals with different densities by

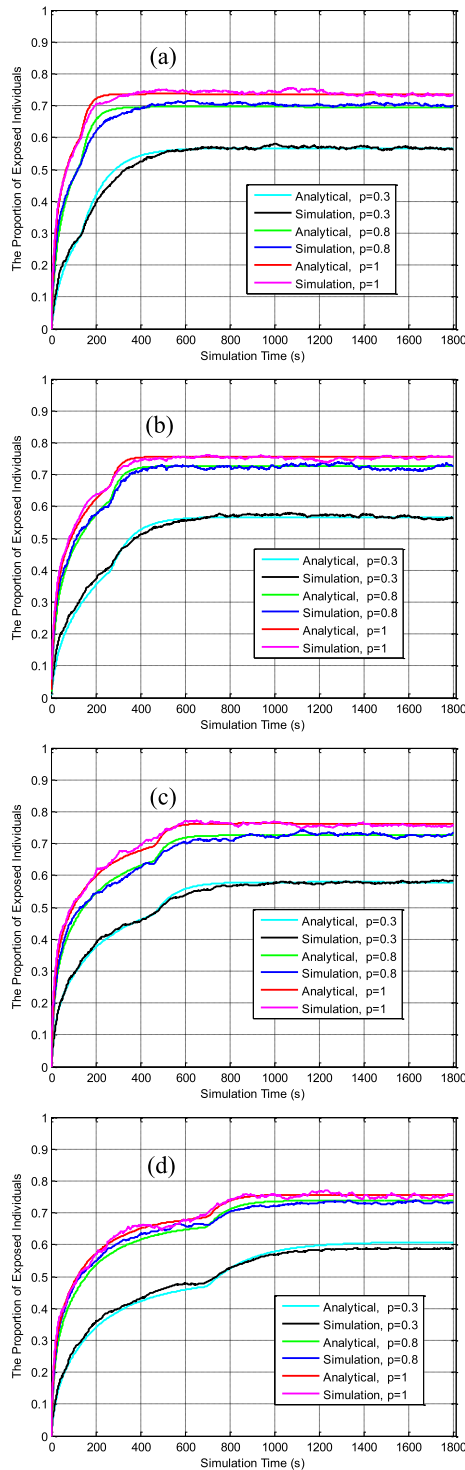


FIGURE 3. Comparisons of the analytical and simulation results with different infected possibilities and densities of individuals. The infection radius of epidemic is 2m, and the region can hold 300, 500, 800, and 1500 individuals at most in (a), (b), (c), and (d), respectively. The exposed rate stabilizes at a certain steady value after the number of individuals reaching the capacity of the region. The exposed rates in (a) firstly stabilize because the number of individuals reaches the capacity of region (i.e. 300) at first.

changing the capacity of the region, the capacity was set to be 300, 500, 800 and 1500, respectively, and the infection radius was uniformly set to be 2m. We can see that improving

TABLE 1. The MAPE (%) and the steady value (SV) of the analytical exposed rate of each simulation scenario in Fig. 3.

Capacity	Possibility $p = 0.3$		Possibility $p = 0.8$		Possibility $p = 1$	
	MAPE	SV	MAPE	SV	MAPE	SV
300	2.01	0.57	3.08	0.70	2.11	0.74
500	2.39	0.57	1.28	0.73	1.05	0.76
800	1.31	0.58	1.35	0.73	1.92	0.76
1500	2.84	0.61	1.98	0.74	1.21	0.76

the prevention level (or reducing the infection possibility) can slow down the epidemic spreading. In each scenario, the exposed rate stabilizes at a steady value (SV, which can reflect the outbreak size of epidemic) in the end. On the same prevention level, the SVs of exposed rates almost are the same regardless of the density of individuals (shown in Table 1), and the SV of exposed rate decreases with the prevention level improving. Especially, the SV of the extreme infection rate is about 0.75 (i.e., not all of the susceptible individuals are infected) due to the susceptible individuals continuously entering the region. In all of the figures, it is obvious that the curves of analytical results are very close to the simulation curves. We used the mean absolute percent error (MAPE) to quantitatively analyze the accuracy of the analytical results obtained by the proposed model. The definition of MAPE is

$$MAPE = \frac{1}{n} \sum_{l=1}^n \left| \frac{\bar{e}_{simulation}(l) - e_{analytical}(l)}{\bar{e}_{simulation}(l)} \right| \times 100\% \quad (5)$$

Where n is the total number of seconds, $\bar{e}_{simulation}(l)$ is the average exposed rate of the 100 repeated simulations at the l^{th} second, and $e_{analytical}(l)$ is the exposed rate calculated by the proposed model at the l^{th} second. The MAPEs of each scenario in Fig. 3 are shown in Table 1. We can see that the MAPEs are smaller than 5% in all of the results. This means that the analytical results obtained by the proposed model well coincide with that of simulation results, and the analytical model can well describe epidemics spread in these scenarios.

Fig. 4(a) shows the results of different epidemics spreading with the infection possibility of 0.3 in the region. We distinguished the epidemics by their infection radii, a larger infection radius represents the epidemic has a higher infection ability. We modeled three kinds of epidemics whose infection radii are 1m, 2m and 3m, respectively. In Fig. 4(a), the capacity of the region was set to be 300, and the three kinds of epidemics independently spread among the individuals. From Fig. 4(a), we can see that the epidemic with lowest infection ability ($r = 1m$) reaches its steady value takes about 1200s, and that spends only about 400s for the most powerful epidemic ($r = 3m$). This means an epidemic with higher infection ability (or larger infection radius) can spread faster

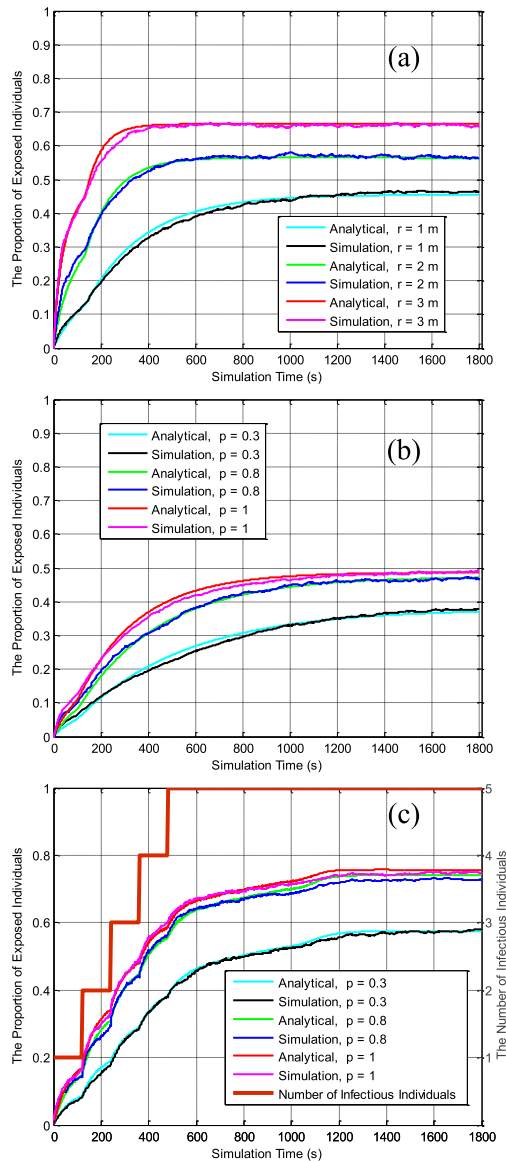


FIGURE 4. Comparisons of the analytical and simulation results under different scenarios. The capacity of the region is 300. (a) The average infected possibility of individuals is 0.3, and the number of infectious individuals is 5 in the whole simulation process. (b) The infection radius of epidemic is 2m, and the number of infectious individuals is 1 in the whole simulation process. (c) The infection radius of epidemic is 2m, and the number of infectious individuals increases from 1 to 5 in the simulation process.

among the individuals. Besides, an epidemic with higher infection ability has a larger SV of exposed rate. The MAPEs are 3.08% ($r = 1\text{ m}$), 2.09% ($r = 2\text{ m}$) and 1.37% ($r = 3\text{ m}$), respectively, which indicates the analytical model can well depict different epidemics spread in open finite regions.

In Fig. 3 and 4(a), the initial number of individuals in the region was uniformly set to be 100, among them 5 were in infectious state and the others were in susceptible state. In Fig. 4(b) and (c), we changed the initial values of the infectious individual number. In Fig. 4(b), we set the number of infectious individuals to be 1 to simulate the epidemic spreading under the condition that the proportion of

infectious individuals is extremely low, and other settings were the same as that in Fig. 3(a). Compared to Fig. 3(a), the speed of epidemic spreading in Fig. 4(b) is much smaller. The SV of the extreme infection ($p = 1$) rate decreases from 0.76 to 0.49, and steady exposed rates of the other two scenarios decreases from 0.57 to 0.37 ($p = 0.3$) and from 0.73 to 0.47 ($p = 0.8$), respectively. This means restricting the infectious individuals to entering can effectively suppress the epidemic spreading in the region. The MAPEs in these scenarios are 2.64% ($p = 0.3$), 2.95% ($p = 0.8$) and 3.32% ($p = 1$), which also demonstrates the proposed model is suitable for describing epidemics spread in these scenarios.

In the aforementioned simulations, in order to observe the effect of single factor on the results, we assumed that 1) all of the arrival individuals were in the susceptible state, and 2) the number of infectious individuals is constant in the whole simulation processes. Therefore, we had $s'(t) = 1$, $e'(t) = 0$ and $i'(t) = 0$ in accordance with these assumptions. In Fig. 4(c), we relaxed these assumptions. We changed one of the initial conditions of the simulation in Fig. 3(a), we set the initial number of the infectious individuals to be 1, and other infectious individuals can enter the region in the simulation process. We allowed 5 infectious individuals entering the region at most. From Fig. 4(c), we can see that when a new infectious individual enters the region, the spread process of epidemic is obviously speeded up. The SVs of exposed rates stay at 0.58 ($p = 0.3$), 0.74 ($p = 0.8$) and 0.76 ($p = 1$) in the end, respectively, which almost are the same as that in Fig. 3. This means the SV of exposed rate of an epidemic mainly relies on the average infected possibility of individuals and the number of infectious individuals in the region. The MAPEs of the results are 1.94% ($p = 0.3$), 2.51% ($p = 0.8$) and 2.32% ($p = 1$), which proves the analytical curves follow the simulation curves very well.

As can be seen from the figures, the analytical and simulation curves are very close. We have presented that the MAPEs of all the results are smaller than 5%, which indicates the proposed model can accurately describe the epidemics spreading in open finite regions. By the way, through comparing the results, we can carefully draw a conclusion that the steady exposed rate of a specific infection disease mainly depends on 1) the average infected possibility of the individuals, 2) the infection ability of the epidemic, and 3) the number of infectious individuals in the region, while the density of individuals has no significant impact on the SV of exposed rate. Furthermore, an epidemic with higher infection ability has a larger SV of exposed rate and spreads faster than one with lower infection ability.

The real-time arrival rate was adopted in the aforementioned results. In Fig. 5, we compared the difference between the real-time and average arrival rates when they are used in the analytical model. Herein, we just showed a part of the results of the simulation scenarios in Fig. 3 (i.e., with average infected possibility of 0.3 in each capacity of the region) due to the space restriction. Since we did not consider the departure rate, for simplicity, the number of the individuals was

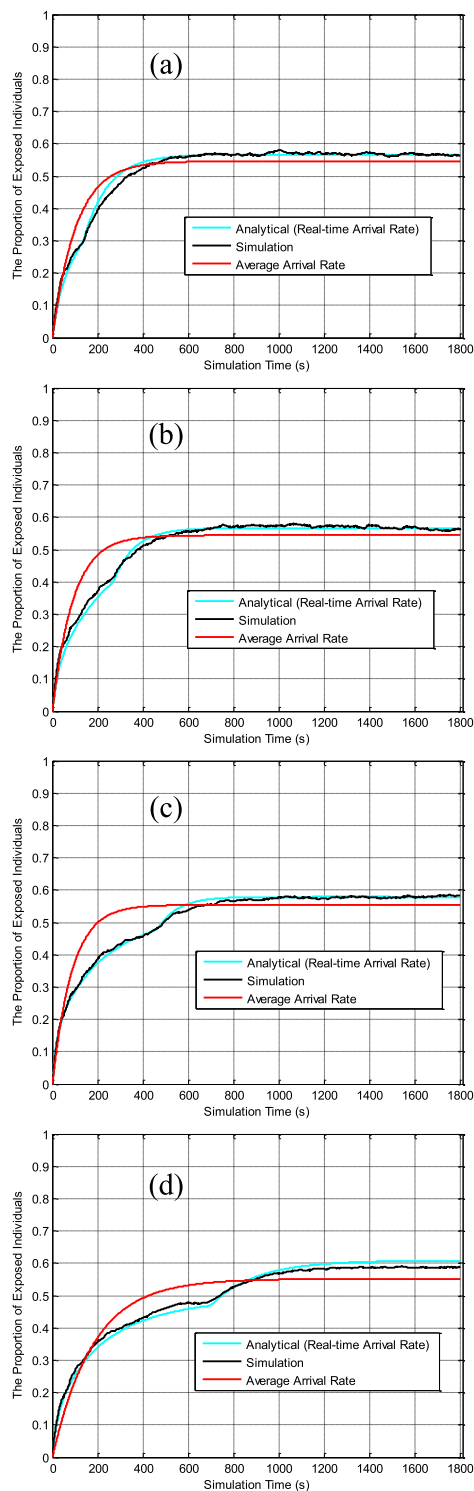


FIGURE 5. Comparisons of the real-time and average arrival rates. The average infected possibility is 0.3; the infection radius is 2m; the number of infectious individuals is 5 in the whole simulation process. The region can hold 300, 500, 800, and 1500 individuals at most in (a), (b), (c), and (d), respectively.

fixed to the capacity of the region when the average arrival rate was adopted. We can see that the analytical curve is closer to the simulation curve when the real-time arrival rate was

TABLE 2. The MAPEs (%) and SVs of analytical exposed rates of the results in Fig. 5.

Arrival rate \ Capacity	300		500		800		1500	
	MAPE	SV	MAPE	SV	MAPE	SV	MAPE	SV
real-time	2.01	0.57	2.39	0.57	1.31	0.58	2.84	0.61
average	6.00	0.55	7.97	0.54	8.76	0.55	8.40	0.55

adopted. The MAPEs are shown in Table 2. When the average arrival rate was adopted, though it cannot well describe the spread of epidemics, the MAPEs are less than 10%, and the SV errors of exposed rates are less than 0.1. Generally, real-time arrival rate is difficult to obtain, but the average arrival rate can be estimated according to the historical data. The results demonstrate that the proposed model with average arrival rate can give a reasonable prediction about the outbreak sizes of epidemics.

IV. CONCLUSION

In this paper, we have presented an analytical model with variable contact rate to describe the spread of epidemics in open finite regions. In the model, we took the variable number of people and the dynamic migration rate into account. We confirmed the validity of proposed model by performing numerical simulations in different scenarios. Through comparing the results in different scenarios, we found that an epidemic with a larger infection radius spreads faster and has a larger SV of exposed rate than one with smaller infection radius. For a specific infection disease, the outbreak size mainly depends on the average infected possibility of the individuals and the number of infectious individuals in the region. The density of individuals has no significant impact on the steady exposed rate. Importantly, our study indicates that two ways can help to suppress epidemics spread in open regions: 1) improving the prevention level to reduce the infected possibility of people, 2) restricting infectious people enter the regions. In the futher research, we will apply the model to evaluate the performance of epidemic routing in the open regions.

REFERENCES

- [1] M. Chen, Y. Ma, Y. Li, D. Wu, and Y. Zhang, "Wearable 2.0: Enabling human-cloud integration in next generation healthcare systems," *IEEE Commun. Mag.*, vol. 55, no. 1, pp. 54–61, Jan. 2017.
- [2] D. Tian, J. Zhou, Y. Wang, H. Xia, Z. Yi, and H. Liu, "Optimal epidemic broadcasting for vehicular ad hoc networks," *Int. J. Commun. Syst.*, vol. 27, no. 9, pp. 1220–1242, 2015.
- [3] D. Tian, J. Zhou, Y. Wang, G. Zhang, and H. Xia, "An adaptive vehicular epidemic routing method based on attractor selection model," *Ad Hoc Netw.*, vol. 36, no. P2, pp. 465–481, 2015.
- [4] T. M. Chen and J. M. Robert, "Worm epidemics in high-speed networks," *Computer*, vol. 37, no. 6, pp. 48–53, Jun. 2004.
- [5] P. T. Eugster, R. Guerraoui, A. M. Kermarrec, and L. Massoulié, "Epidemic information dissemination in distributed systems," *Computer*, vol. 37, no. 5, pp. 60–67, May 2004.
- [6] S. Yan, S. Tang, and W. Fang, "Global and local targeted immunization in networks with community structure," *J. Statist. Mech. Theory Experim.*, vol. 2015, no. 8, p. 08010, 2015.

- [7] P.-Y. Chen, S.-M. Cheng, and K.-C. Chen, "Optimal control of epidemic information dissemination over networks," *IEEE Trans. Cybern.*, vol. 44, no. 12, pp. 2316–2328, Dec. 2014.
- [8] M. Y. Li, J. R. Graef, L. Wang, and J. Karsai, "Global dynamics of a seir model with varying total population size," *Math. Biosci.*, vol. 160, no. 2, pp. 191–213, 1999.
- [9] H. F. Zhang, Z. X. Wu, and M. Tang, "Effects of behavioral response and vaccination policy on epidemic spreading—An approach based on evolutionary-game dynamics," *Sci. Rep.*, vol. 4, pp. 1–10, Apr. 2013.
- [10] T. Liu, Y. Zhang, and H. Lin, "A large temperature fluctuation may trigger an epidemic erythromelalgia outbreak in China," *Sci. Rep.*, vol. 5, pp. 1–8, Apr. 2015.
- [11] C. J. Worby, C. Kenyon, and R. Lynfield, "Examining the role of different age groups, and of vaccination during the 2012 minnesota pertussis outbreak," *Sci. Rep.*, vol. 5, pp. 1–8, Oct. 2015.
- [12] D. Guo, K. C. Li, and T. R. Peters, "Multi-scale modeling for the transmission of influenza and the evaluation of interventions toward it," *Sci. Rep.*, vol. 5, pp. 1–9, Oct. 2015.
- [13] V. S. Del, H. Hethcote, J. M. Hyman, and C. Castillochavez, "Effects of behavioral changes in a smallpox attack model," *Math. Biosci.*, vol. 195, no. 2, pp. 228–251, 2005.
- [14] L. Pappalardo, F. Simini, and S. Rinzivillo, "Returners and explorers dichotomy in human mobility," *Nature Commun.*, vol. 6, nos. 1–8, Sep. 2015.
- [15] J. M. Epstein, "Modelling to contain pandemics," *Nature*, vol. 460, no. 6, p. 687, 2009.
- [16] V. Colizza and A. Vespignani, "Epidemic modeling in metapopulation systems with heterogeneous coupling pattern: Theory and simulations," *J. Theor. Biol.*, vol. 251, no. 3, pp. 450–467, 2008.
- [17] V. Colizza, R. Pastor-satorras, and A. Vespignani, "Reaction-diffusion processes and metapopulation models in heterogeneous networks," *Nature Phys.*, vol. 3, no. 4, pp. 276–282, 2007.
- [18] S. Jone, "Continuous-time formulation of reaction-diffusion processes on heterogeneous metapopulations," *Phys. Rev. E, Stat. Phys. Plasmas Fluids Relat. Interdiscip. Top.*, vol. 78, no. 1, pp. 1–4, 2008.
- [19] M. Chen, P. Zhou, and G. Fortino, "Emotion communication system," *IEEE Access*, vol. 5, pp. 326–337, Apr. 2017.
- [20] M. Chen, J. Yang, Y. Hao, S. Mao, and K. Hwang, "A 5G cognitive system for healthcare," *Big Data Cognit. Comput.*, vol. 1, no. 1, pp. 1–2, 2017.
- [21] L. Hébert-Dufresne, A. Allard, and J. G. Young, "Global efficiency of local immunization on complex networks," *Sci. Rep.*, vol. 3, pp. 1–8, May 2013.
- [22] D. Balcan, V. Colizza, and B. Gonçalves, "Multiscale mobility networks and the spatial spreading of infectious diseases," *Proc. Nat. Acad. Sci. USA*, vol. 106, no. 51, pp. 21484–21489, 2009.
- [23] P. Holme, "Information content of contact-pattern representations and predictability of epidemic outbreaks," *Sci. Rep.*, vol. 5, pp. 1–12, Apr. 2015.
- [24] C. Poletto, S. Meloni, and M. A. Van Metre, "Characterising two-pathogen competition in spatially structured environments," *Sci. Rep.*, vol. 5, pp. 1–9, May 2014.
- [25] V. Colizza, A. Barrat, and M. Barthélemy, "Modeling the worldwide spread of pandemic influenza: Baseline case and containment interventions," *PLoS Med.*, vol. 4, no. 1, pp. 1–16, 2007.
- [26] A. Wesolowski, G. Stresman, N. Eagle, and J. Stevenson, "Quantifying travel behavior for infectious disease research: A comparison of data from surveys and mobile phones," *Sci. Rep.*, vol. 4, pp. 1–7, Sep. 2014.
- [27] A. Lima, D. M. De, V. Pejovic, and M. Musolesi, "Disease containment strategies based on mobility and information dissemination," *Sci. Rep.*, vol. 5, pp. 1–13, Sep. 2014.
- [28] L. Bengtsson *et al.*, "Using mobile phone data to predict the spatial spread of cholera," *Sci. Rep.*, vol. 5, pp. 1–5, Sep. 2015.
- [29] Y. Gu *et al.*, "Early detection of an epidemic erythromelalgia outbreak using Baidu search data," *Sci. Rep.*, vol. 5, pp. 1–10, Jul. 2015.
- [30] W. B. Du, X. L. Zhou, O. Lordan, Z. Wang, C. Zhao, and Y. B. Zhu, "Analysis of the Chinese airline network as multi-layer networks," *Transp. Res. E Logistics Transp. Rev.*, vol. 89, pp. 108–116, Apr. 2016.
- [31] V. Colizza and A. Vespignani, "Invasion threshold in heterogeneous metapopulation networks," *Phys. Rev. Lett.*, vol. 99, no. 14, pp. 1–4, 2008.
- [32] H. Yang, M. Tang, and T. Gross, "Large epidemic thresholds emerge in heterogeneous networks of heterogeneous nodes," *Sci. Rep.*, vol. 5, pp. 1–12, Apr. 2015.
- [33] M. Chen, Y. Ma, J. Song, C. F. Lai, and B. Hu, "Smart clothing: Connecting human with clouds and big data for sustainable health monitoring," *Mobile Netw. Appl.*, vol. 21, no. 5, pp. 825–845, 2016.
- [34] J. Anders, H. Dirk, Z. A. Habib, and A. Salim, "From crowd dynamics to crowd safety: A video-based analysis," *Adv. Complex Syst.*, vol. 11, no. 4, pp. 497–527, 2011.
- [35] C. Poletto, M. Tizzoni, and V. Colizza, "Heterogeneous length of stay of hosts' movements and spatial epidemic spread," *Sci. Rep.*, vol. 2, pp. 1–11, Apr. 2012.
- [36] H. Hu, K. Nigmatulina, and P. Eckhoff, "The scaling of contact rates with population density for the infectious disease models," *Math. Biosci.*, vol. 244, pp. 125–134, Sep. 2013.
- [37] L. Goscé, D. A. Barton, and A. Johansson, "Analytical modelling of the spread of disease in confined and crowded spaces," *Sci. Rep.*, vol. 4, no. 18, pp. 1–6, 2014.
- [38] M. Munizaga, F. Devillaine, C. Navarrete, and D. Silva, "Validating travel behavior estimated from smartcard data," *Transp. Res. C, Emerg. Technol.*, vol. 44, no. 4, pp. 70–79, 2014.
- [39] S. Tao, D. Rohde, and J. Corcoran, "Examining the spatial-temporal dynamics of bus passenger travel behaviour using smart card data and the flow-comap," *J. Transp. Geogr.*, vol. 41, no. 41, pp. 21–36, 2014.
- [40] T. Kusakabe and Y. Asakura, "Behavioural data mining of transit smart card data: A data fusion approach," *Transp. Res. C, Emerg. Technol.*, vol. 46, pp. 179–191, Sep. 2014.
- [41] C. Bettstetter, "Mobility modeling in wireless networks: Categorization, smooth movement, and border effects," *ACM SIGMOBILE Mobile Comput. Commun. Rev.*, vol. 5, no. 3, pp. 55–66, 2001.



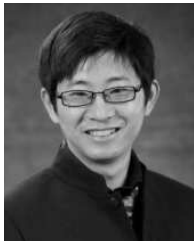
DAXIN TIAN is currently a Professor with the School of Transportation Science and Engineering, Beihang University, Beijing, China. His current research interests include mobile computing, intelligent transportation systems, vehicular ad hoc networks, and swarm intelligence.



CHAO LIU is currently pursuing the degree with the School of Transportation Science and Engineering, Beihang University, Beijing, China. His current research focuses on Vehicle-to-X communication systems.



ZHENGGUO SHENG is currently a Lecturer with the Department of Engineering and Design, University of Sussex, U.K. His current research interests are focused on cloud computing, Internet of Things, machine-to-machine, power line communications, vehicle communications, and wireless sensor networks.



MIN CHEN is currently a Professor with the School of Computer Science and Technology, Huazhong University of Science and Technology, Wuhan, China. His research interests include cyber physical systems, IoT sensing, 5G networks, mobile cloud computing, SDN, health care big data, medical cloud privacy and security, body area networks, and emotion communications and robotics.



YUNPENG WANG is currently a Professor with the Beijing Key Laboratory for Cooperative Vehicle Infrastructure Systems and Safety Control, School of Transportation Science and Engineering, Beihang University, Beijing, China. His current research interests include intelligent transportation systems, traffic safety, and vehicle infrastructure integration.

...